

Coherence of persistent currents in multiwall carbon nanotubes

M. Szopa, M. Margańska, E. Zipper, and M. Lisowski

Department of Theoretical Physics, University of Silesia, ul Uniwersytecka 4, 40 007 Katowice, Poland

(Received 4 February 2004; revised manuscript received 27 April 2004; published 11 August 2004)

Persistent currents in multiwalled carbon nanotubes (MWNT's), driven by the magnetic field parallel to the tube axis are studied. The geometrical structure and possibility of the existence of MWNT's with shells in various chiral configurations are explored. The currents are calculated considering a possible Fermi energy shift by hole doping. The influence of self-inductance of different shells is taken into account. The optimal chiralities for the maximal current are found to be the armchair-only configuration (A) without doping and the zig-zag-chiral-chiral-zig-zag configuration ((B) and (C)) doped to $E_F = -\gamma$ ($\gamma = 3.033$ eV is the hopping integral between graphene sites). The hole doped (B) configurations are shown to exhibit spontaneous currents in Kelvin temperatures. In the optimal diamagnetic configuration (C) a Meissner-type effect, i.e., partial flux expulsion, occurs.

DOI: 10.1103/PhysRevB.70.075406

PACS number(s): 73.22.-f, 73.23.Ra

I. INTRODUCTION

Carbon nanotubes (henceforth referred to as CN's) can play a major role in the design of the next-generation nano-electronic and nanoelectromechanical devices due to their novel mechanical and electronic properties. Among many other fascinating features,¹ carbon nanotubes have a topology which makes them particularly fit to investigate the phenomenon of persistent currents in the presence of static magnetic field. In one of our earlier papers we studied persistent currents in pure and hole-doped single-wall nanotubes (SWNT's).² We have shown that the shape of the Fermi surface changes with the doping, which influences the amplitude and form of the persistent currents, and that the amplitudes of the currents and their associated magnetic moments were small. However, we know from the study of mesoscopic systems that they might increase with increasing number of transverse channels. In this paper we investigate persistent currents in MWNTs, driven by an external magnetic field parallel to the tube axis. These currents are a superposition of currents from different shells. Thus, the overall current can be significantly enhanced in those MWNTs where the currents from different shells add constructively, i.e., when they display the same paramagnetic or diamagnetic behaviour. However, different shells in MWNTs have in general different chiralities and the question arises whether we can find such favourable tube configurations.

We have performed model calculations for several possible configurations among which we found some which indeed yielded large currents. We can then assume that the magnetic flux is the sum of the external flux and the flux coming from the currents themselves. We arrive at the self-consistent equation for the flux which can have spontaneous solutions,³ i.e., a current running in the absence of the external field. Such spontaneous solutions appear when the currents are paramagnetic. If the currents from different shells are diamagnetic, the MWNT can exhibit at least a partial flux expulsion.⁵

The influence of self-inductance of individual layers on the currents flowing in the remaining ones is also taken into

account in our calculations. Both the effects of mutual and self-inductance on persistent currents have been studied, in mesoscopic rings and cylinders, by the authors of Refs. 3 and 4. In this paper we apply these ideas to multiwall CN's, in order to find out whether collective phenomena are possible in these systems. We are going to investigate both pure and hole-doped (where the Fermi level is shifted below its neutral position) MWNTs. Depending on the method of doping used there are at least two distinct cases to consider: one, where only the outer shell is doped, and the other, where the Fermi surface of every shell is lowered. We study mainly the nanotubes doped by the electrochemical method, as it allows us to achieve largest shifts of the Fermi level.⁶ Since this method involves immersing a nanotube in the electrolyte, we assume that all shells are in contact with this medium, and that the Fermi level is shifted to the same value in all shells of the multiwall nanotube.

This paper is organized as follows: We start from considering the geometry of a multiwall nanotube. For some chiralities the currents should be greatly enhanced, for others, dampened.² In Sec. II we investigate the possible chiralities of the shells of a MWNT. We take into account the D_6 invariance of the honeycomb lattice and the restrictions stemming from the existence of an optimal distance between nanotube shells. We also indicate the configurations which would yield the most stable and enhanced persistent currents.

In Sec. III the details of the calculation of persistent currents in CNs are presented. In Sec. IV we consider the possible effects of the flux induced by the current in each tube on the persistent currents flowing in the remaining ones. Analytical expressions for these self-inductance contributions to the flux are provided, and numerical simulations performed for a few chirality configurations.

In Sec. V we study the behavior of multiwall CNs with and without a hole doping. We calculate the persistent currents flowing in MWNTs with optimal chirality configurations and investigate the possible appearance of spontaneous current and of partial flux expulsion.

II. GEOMETRICAL STRUCTURE OF A MULTIWALL NANOTUBE

The carbon nanotubes inherit many properties of graphite, their generic material. Among those is the optimal distance between nanotube shells, which is close to the distance between graphene sheets in turbostratic graphite, i.e., $\approx 3.44 \text{ \AA}$.⁷ The curvature of the tube introduces a deviation from this optimum distance, and in small nanotubes shell separation can differ quite significantly from its value in graphite. However in this paper we are working on wide nanotubes, where these effects are negligible,¹ and we can safely assume that the neighbouring shells of the tube are $d = 3.44 \text{ \AA} \pm \Delta d$ apart, where Δd is a small deviation of the distance between shells. This restriction imposes some conditions on the chiralities of the shells.

Let us consider a MWNT whose shells are defined by the circumference vectors $\mathbf{L}_i = m_i \mathbf{T}_1 + n_i \mathbf{T}_2$, where \mathbf{T}_1 , \mathbf{T}_2 are the generators of the graphene's honeycomb lattice,² the length of \mathbf{L}_i is $L_i = a_{C-C} \sqrt{3(m_i^2 + m_i n_i + n_i^2)}$, and $a_{C-C} = 1.42 \text{ \AA}$ is the length of a C–C bond. Let us assume that the first shell has circumference L_1 . The condition for the circumferences of the outer shells is

$$|L_i - (L_1 + (i-1)d)| \leq \Delta d. \quad (1)$$

The resulting formula for the parameters of such a tube is

$$n_i + \frac{m_i}{2} \pm \sqrt{\left(\frac{L_1 + (i-1)d}{\sqrt{3}a_{CC}}\right)^2 - \frac{3m_i^2}{4}} \leq \frac{\Delta d}{a_{CC}}. \quad (2)$$

It gives all possible combinations of m_i and n_i parameters. However, because of the symmetry of the honeycomb lattice, each pair (m_i, n_i) is geometrically equivalent to five others. The equivalence relation in question is the rotation of the graphene plane by $\pi/3$, identifying the points with coordinates:

$$\begin{aligned} (m_i, n_i) &\rightarrow (-n_i, m_i + n_i) \rightarrow (-m_i - n_i, m_i) \rightarrow (-m_i, -n_i) \\ &\rightarrow (n_i, -m_i - n_i) \rightarrow (m_i + n_i, -m_i). \end{aligned} \quad (3)$$

The plot of possible pairs (m_i, n_i) (marked by open dots in Fig. 1) for three shells of a multiwall nanotube grown around a central $(m_1, n_1) = (12, 0)$ ($R_1 = 4.7 \text{ \AA}$) or $(m_1, n_1) = (7, 7)$ ($R_1 = 4.75 \text{ \AA}$) one is shown in Fig. 1. We assume that $\Delta d = 0.1 \text{ \AA}$.

While studying SWNTs sometimes only those where $m \geq n$ are taken into account, since a single (n, m) nanotube is the inverse image of a (m, n) one and has the same properties as a (m, n) nanotube but with the direction of the flux reversed. In multiwall nanotubes however the inverse shells produce inverse currents ($I_{(m,n)}(\phi) = -I_{(n,m)}(\phi)$) which change the total current.

In Fig. 1 are marked the (m_i, n_i) pairs which belong to the unique 1/6th of the total number of possible parameters. The armchair shells lie on the $n_i = m_i$ line (dashed line in Fig. 1), while those on the m_i axis represent tubes with zig-zag chiralities. The stars denote the chiralities of the shells in an arbitrary configuration whose inner and outer shells are zig-zag nanotubes of the same parity and the black dots—the chiralities in a MWNT with armchair shells only. Note that

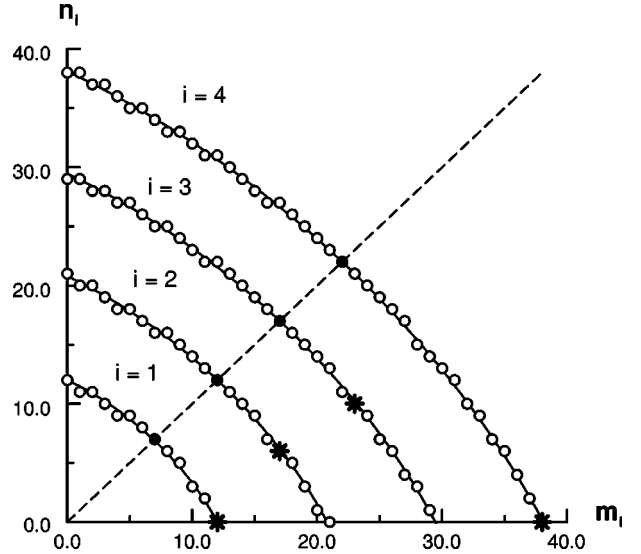


FIG. 1. The plot of m_i vs n_i for four shells of a nanotube, whose inner shell has the radius $R_1 = 4.7 \pm 0.1 \text{ \AA}$, corresponding to $L_1 = 29.5 \text{ \AA}$, where we assume $\Delta d = 0.1 \text{ \AA}$.

for the third shell there is no suitable zig-zag nanotube, while allowed armchair configurations exist for all shells.

Our aim is to obtain the maximum enhancement of the persistent current in MWNT, coming from the supersposition of currents from different shells. Therefore we shall consider the suitable chirality configurations. From earlier work² we know that zig-zag SWNTs doped to the $E_F = -\gamma$ (where $\gamma = 3.033 \text{ eV}$ is the hopping integral between two graphene sites) display strongly enhanced currents. Undoped armchair nanotubes exhibit smaller, but still considerable currents. Due to the structure of the Brillouin zone, the persistent currents in doped zig-zag nanotubes are either diamagnetic (when m is odd) or paramagnetic (when m is even). Therefore we choose configurations which contain zig-zag shells of the same parity. In Table I, examples of such chirality configurations with corresponding mean distances between shells are shown.

The first two configurations containing zig-zag nanotubes do not meet our requirements, since their zig-zag shells either have different parities or the intershell distance differs too much from d . The third zig-zag configuration [of the type $(m_1, 0)(m_1 + 26, 0)$] both maintains the graphite distance between nanotube shells and contains zig-zag shells of the same parity. It contains two chiral nanotubes between each pair of zig-zag shells. As regards the armchair configuration, we are in the best possible situation, since from the geometrical point of view it is possible to obtain a multiwall nanotube containing only armchair shells. Pure armchair nanotubes always exhibit paramagnetic current, regardless of their parity. In the following we shall consider in detail these two cases: armchair (undoped) and zig-zag (doped to $E_F = -\gamma$) tubes.

III. PERSISTENT CURRENTS IN NARROW MWNT'S

In our model, at $T=0$ the persistent current in a single, i th shell of the MWNT is given by the formula

TABLE I. Chirality configurations with corresponding mean distances between shells.

| Inner shell | Configuration type | Outer zig-zag or armchair parameters | intershell distance |
|-------------------------|-------------------------------|--------------------------------------|---------------------|
| zig-zag ($m_1, 0$) | zig-zag-zig-zag | $(m_1+8, 0)$ | 3.13 Å |
| | | $(m_1+9, 0)$ | 3.52 Å |
| | zig-zag-chiral-zig-zag | $(m_1+17, 0)$ | 3.32 Å |
| | | $(m_1+18, 0)$ | 3.62 Å |
| | zig-zag-chiral-chiral-zig-zag | $(m_1+26, 0)$ | 3.39 Å |
| | | $(m_1+27, 0)$ | 3.73 Å |
| armchair (m_1, m_1) | armchair, armchair | (m_1+5, m_1+5) | 3.39 Å |

$$I_i(\phi_i) = \sum_{\mathbf{k}_i \text{ occupied}} I_i(\mathbf{k}_i, \phi_i) = \sum_{\mathbf{k}_i \text{ occupied}} -\frac{\partial E(\mathbf{k}_i)}{\partial \phi_i}, \quad (4)$$

where \mathbf{k}_i is the momentum of an individual electron state, $E(\mathbf{k}_i)$ is the dispersion relation of a graphene lattice in the i th shell, and ϕ_i is the flux in the tube. The sum runs over all occupied momentum states in the Brillouin zone, and depends on the level of doping achieved in the nanotube. In nonzero temperature, the total current being a sum of individual shell currents is calculated from the minimum of the free energy,³

$$I_i(\phi_i, T) = \sum_i \sum_{\mathbf{k}_i} \frac{-1}{1 + e^{[(E(\mathbf{k}_i) - \mu(\phi_i))/kT]}} \frac{\partial E(\mathbf{k}_i)}{\partial \phi_i}, \quad (5)$$

where ϕ_i is the total flux through the nanotube, equal to the flux in the outermost shell. Since the shells of the nanotube are close enough to exchange electrons,⁸ the chemical potential $\mu(\phi_i)$ is common for all of them. It can be calculated from the condition

$$\sum_i \sum_{\mathbf{k}_i} \frac{1}{1 + \exp\{(E(\mathbf{k}_i) - \mu(\phi_i))/kT\}} = N_e, \quad (6)$$

where N_e is the total number of electrons in all the shells of the nanotube, which we assume to be constant.

Depending on the chirality of the shell, its persistent current may be paramagnetic, or diamagnetic. We found that in most configurations the currents in the shells are small or add destructively, resulting in a very small net current. Nevertheless, it is possible to find such configurations that the currents both are large and add coherently, leading to interesting results like possible spontaneous current and partial flux expulsion. The two configurations found in the previous section, doped zig-zag and pure armchair MWNTs, show a large enhancement of the current.

Figures 2 and 3 represent the persistent currents running in each shell of two nanotube configurations—an armchair-only configuration without doping (Fig. 2) and one with two zig-zag walls of the same parity, hole-doped to $E_F = -\gamma$ (Fig. 3). So far there are reports about experimentally obtained

doping to $-1 \text{ eV} \approx -1/3\gamma$,⁹ but further lowering of the Fermi level could also be achieved—such situation has already been considered.¹⁰

The flux on the ϕ_1/ϕ_0 axis is the one in the innermost nanotube. The flux felt by the i th shell is $\phi_1 \cdot s_i/s_1$, hence the periods of currents from individual shells, shown in Figs. 2 and 3 are different.

In an armchair-only configuration (A) all shells give contributions of the same kind (here, paramagnetic), scaling only with the inverse radius of the shell.

| (m_i, n_i) | shell type | diameter in Å |
|--------------|------------|---------------|
| (7, 7) | armchair | 9.4 |
| (12, 12) | armchair | 16.2 |
| (17, 17) | armchair | 23 |
| (22, 22) | armchair | 29.8 |

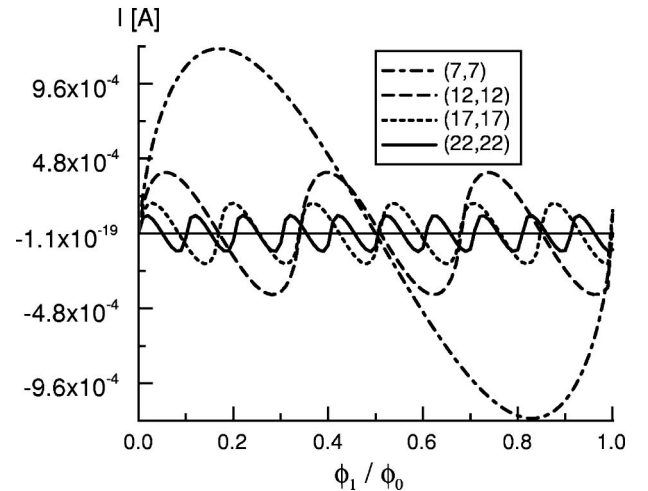


FIG. 2. The case of an armchair-only (A) configuration (black dots in Fig. 1). $E_F = 0$, $T = 1 \text{ K}$. The length of the nanotube is $0.1 \mu\text{m}$, the number of electrons in the whole CN $N_e = N_{\text{half-filling}} = 47144$. All shells contribute to the total current.

| (m_i, n_i) | shell type | diameter in Å |
|--------------|-------------|---------------|
| (12, 0) | even zigzag | 9.4 |
| (17, 6) | chiral | 16.2 |
| (23, 10) | chiral | 22.9 |
| (38, 0) | even zigzag | 29.7 |

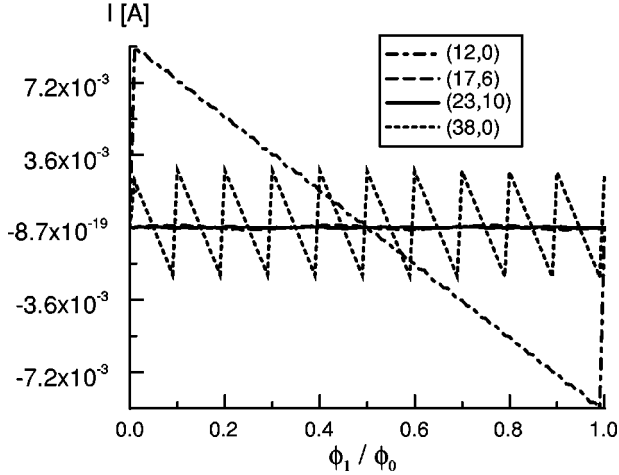


FIG. 3. The case of an optimal zig-zag configuration (B) (stars in Fig. 1). $E_F = -\gamma$, $T = 1\text{K}$. The length of the nanotube is $0.1\ \mu\text{m}$, the number of electrons in the whole CN $N_e = 3/4 N_{\text{half-filling}} = 35114$. The only significant currents are produced by the zig-zag shells, as we expected. Currents from the two chiral shells overlap with the ϕ_1/ϕ_0 axis.

In the second case (B) the paramagnetic (m is even) contributions from the zig-zag shells are dominant (we call them active shells) and from the others negligible. The strong enhancement of the currents in zig-zag shells at $E_F = -\gamma$ doping is due to the structure of the Fermi surface (FS) and momentum spectrum.² The FS is reduced to a smaller hexagone, whose vertices lie at the centers of the edges of the first Brillouin zone. The alignment of the allowed momentum states is now parallel to the edges of the FS, and the jumps in persistent current at integer ϕ/ϕ_0 values occur now for a whole line of momentum states. The resulting current, as could be seen in the Fig. 3, resembles closely that in a mesoscopic metallic ring.¹¹ The shape of the current in a mesoscopic ring with odd or even number of electrons is the same as that of a current in $-\gamma$ -doped zig-zag defined by, respectively, odd or even m parameter.

In the case (B) the currents from active shells add coherently and the total current, being the superposition of currents from all shells, is therefore significantly enhanced. Similar situation occurs in a nanotube with zig-zag walls defined by odd m parameter [configuration (C)], but the currents in this case are diamagnetic. This configuration will be considered in more detail in Sec. V.

IV. THE EFFECT OF SELF-INDUCTANCE OF MWNT SHELLS

In a uniform magnetic field every shell of a MWNT is affected by a slightly different flux. This is due mostly to the fact that every component tube has a different cross section. Moreover, the currents in each shell induce additional flux, felt by all other shells. This flux is proportional to the self-inductance of the shell, \mathcal{L}_i , which we take to be that of a cylinder

$$\mathcal{L}_i = \mu_0 \frac{\pi R_i^2}{L_i}, \quad (7)$$

where R_i is the radius of the i th nanotube, and L_i is its length. For a nanotube composed of n shells, the formulas for the value of the magnetic flux in each shell are the following:

$$\phi_1 = Bs_1 + \mathcal{L}_1 I_1(\phi_1) + \frac{s_1}{s_2} \mathcal{L}_2 I_2(\phi_2) + \cdots + \frac{s_1}{s_n} \mathcal{L}_n I_n(\phi_n),$$

$$\phi_2 = Bs_2 + \mathcal{L}_1 I_1(\phi_1) + \mathcal{L}_2 I_2(\phi_2) + \cdots + \frac{s_2}{s_n} \mathcal{L}_n I_n(\phi_n),$$

...

$$\phi_n = Bs_n + \mathcal{L}_1 I_1(\phi_1) + \mathcal{L}_2 I_2(\phi_2) + \cdots + \mathcal{L}_n I_n(\phi_n), \quad (8)$$

where B is the external magnetic field, ϕ_i is the magnetic flux in the i th shell, counting from the innermost one, $\phi_n = \phi_t$ is the total flux in the MWNT, s_i is the cross section of the i th shell, and I_i its persistent current. It follows from Eq. (8) that the flux in any shell can be expressed as a sum of contributions from inner shells, therefore the flux through in the i th shell of the nanotube is given by

$$\phi_i = \frac{s_i}{s_{i-1}} \phi_{i-1} - \frac{s_i - s_{i-1}}{s_{i-1}} \sum_{j=1}^{j=i-1} \mathcal{L}_j I_j(\phi_j), \quad (9)$$

In order to estimate the magnitude of the self-inductance contribution of the nanotube shells we have first calculated numerically the flux in the outer shell without considering the self-inductance effects, and then with those effects taken into account. In Figs. 4 and 5 we show the self-inductance contribution to the total flux in an armchair-only MWNT.

The oscillatory behavior of the total flux in Fig. 4 and the ratio of the total flux with effects of self-inductance to the total flux without them in Fig. 5 is due to the large number of shells which contribute to the total flux. In small external fields the induced currents are substantial enough for the second term in Eq. (10) to be greater than the first term. Therefore some shells can feel reverse flux. Depending on how many of them are in this diamagnetic regime, the total flux can also be reversed. This fact hints at some self-consistent equations for the magnetic flux in the nanotube, with possible spontaneous solutions. This behavior occurs only for very small flux. As the external field increases, the contribution from self-inductance, compared to the external flux becomes negligible and the flux ratio in Fig. 5 converges to 1.

We have performed our estimate of the self-inductance contributions for nanotubes of approx. 44 nm in diameter.

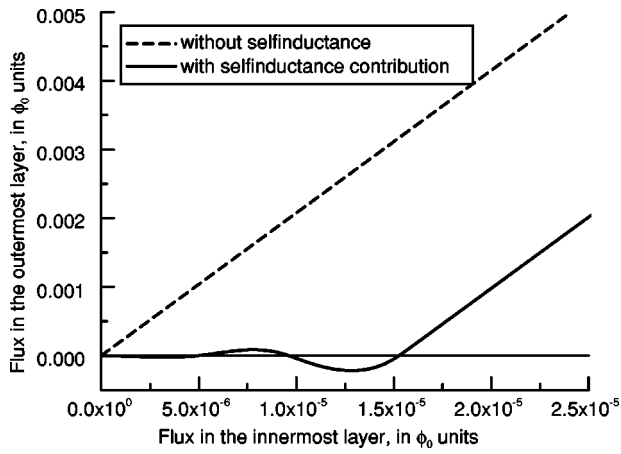


FIG. 4. The flux in the outer shell vs flux in the innermost shell, in a nanotube in (A) configuration, with inner radius $R_1=15 \text{ \AA}$, and outer radius $R_2=221 \text{ \AA}$. $T=0.01 \text{ K}$.

This contribution, $\mathcal{L}I(\phi)$, is linear in nanotube radius, therefore its effect is less pronounced in smaller tubes but larger in wider ones.

V. POSSIBLE COLLECTIVE EFFECTS IN MWNTS

In this section we consider the optimal chirality configurations [(A), (B), and (C)] found in Sec. III and show that the enhanced current can lead to interesting effects. According to Eq. (8) the total flux in the system is

$$\phi_t = \phi_e + \sum_i \mathcal{L}_i I_i(\phi_i), \quad (10)$$

where $\phi_e = Bs_n$ is the external magnetic flux. Let us consider first the MWNT in which the current given by Eq. (5) is paramagnetic [cases (A) and (B)]. The Equation (10) can be written as

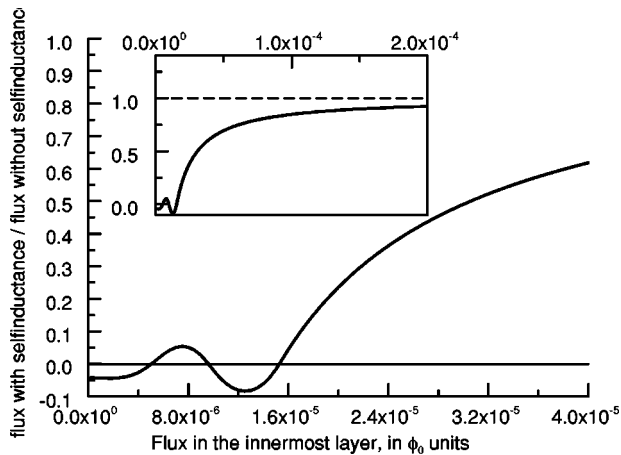


FIG. 5. The ratio of magnetic flux in the outer shell of the multiwall from Fig. 4, with and without self-inductance effects considered. $T=0.01 \text{ K}$.

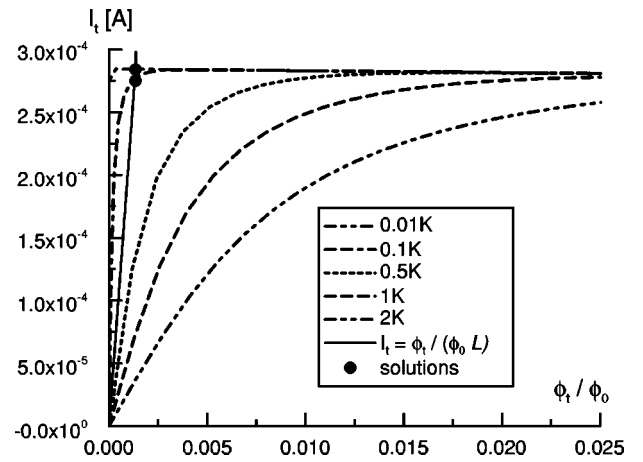


FIG. 6. The total persistent current in an undoped MWNT in configuration (A), for several values of T . Inner radius $R_1=15 \text{ \AA}$, outer radius $R_2=90 \text{ \AA}$, length $L=219 \text{ \AA}$. The MWNT contains 22 armchair shells. The straight line corresponds to Eq. (11) at $\phi_e=0$.

$$\phi_t = \phi_e + \mathcal{L}I_t(\phi_t), \quad (11)$$

where $I_t(\phi_t) = \sum_i I_i(\phi_i)$ and $(\sum_i \mathcal{L}_i I_i(\phi_i)) / I_t(\phi_t)$ is approximated by a constant \mathcal{L} . Equations (5) and (11) form a set of two self-consistent equations for the current.

If Eqs. (5) and (11) have stable, nonvanishing solutions at $\phi_e=0$, they correspond to a spontaneous current appearing in the nanotube, determined by the nonzero intersection of these two functions³ (black dots in Figs. 6 and 7).

The first configuration, (A) is the one containing undoped armchair nanotubes only. They all produce currents of the same, paramagnetic, character and significant amplitude, which add constructively (see Fig. 6). Although the separate currents are all sinusoidal, their superposition has the sawtooth shape which favours the appearance of spontaneous currents. The straight line given by Eq. (11) in the absence of the magnetic flux and the persistent current given by Eq. (5)

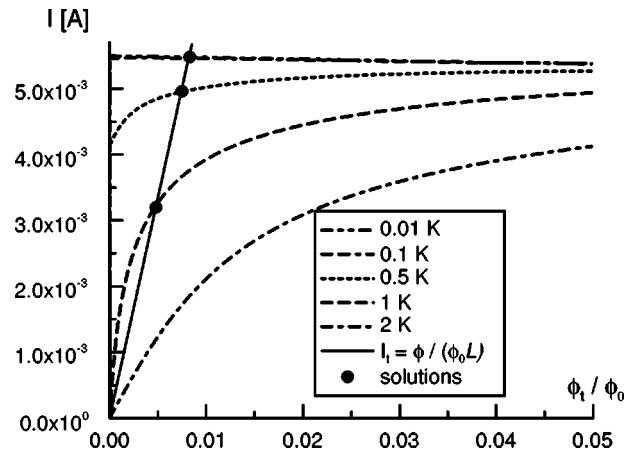


FIG. 7. The currents in a MWNT in configuration (B) with 18 active shells (and 34 inactive chiral ones), for several values of T , with inner radius $R_1=16 \text{ \AA}$, outer radius $R_2=199 \text{ \AA}$, and length $L=426 \text{ \AA}$, at $E_F = -\gamma$ doping. Black dots denote stable solutions.

have nonzero intersections below $T=0.2$ K, corresponding to a spontaneous current $I_t \approx 2.8 \cdot 10^{-4}$ A.

In cases (B) and (C) we calculate the persistent currents in nanotubes where electron density is less than one electron per atom, i.e., which have been hole-doped. The configuration (B) contains zig-zag nanotubes of the same, even, parity, all doped to $E_F = -\gamma$ level (Fig. 7). Because of the inactive shells the nanotube is larger than the one in (A) configuration, its outer shells have greater self-inductance. Since the length of this nanotube is twice the length of the previous one, the amplitude of the currents is doubled. Moreover, the effect of the flat Fermi surface is so large that the amplitude of the currents is in total ≈ 20 times larger than in the previous case, although there are fewer active sheets. Here the spontaneous current in the nanotube can appear already at $T \lesssim 1$ K. At $T=0.01$ K it is of the order $5.5 \cdot 10^{-3}$ A.

We are now in a position to compare our model calculations for the configurations (A) and (B). From Figs. 6 and 7 we see that the zig-zag case, because of the larger amplitude of $I_t(\phi_t)$, is more likely to allow some nontrivial solutions with spontaneous current than the armchair case. Since the amplitude of the current in one shell of the MWNT is inversely proportional to its radius, the largest contribution to the overall current comes from the innermost shell. In the case (A) its amplitude is $7.12 \cdot 10^{-5}$ A and the currents from the remaining shells enhance the overall current by a factor of 4. For zig-zag configuration the amplitude of the current in the innermost shell is about $1.3 \cdot 10^{-3}$ A, so an enhancement by a factor of ≈ 4 is achieved as well, but the current has a larger amplitude. This case is the most favourable for the appearance of a spontaneous current at low temperatures.

In the model considerations presented in Figs. 6 and 7 we set the length of the nanotube to be rather small in order to reduce the time of computer calculations. However, from these results we can estimate the results for longer tubes. Real nanotubes can be two orders of magnitude longer resulting in proportional increase of the persistent currents. Since the self-inductance is inversely proportional to the nanotube length, the spontaneous currents will also increase by two orders of magnitude, i.e., in case of $L \approx 1 \mu\text{m}$ they can be of the order of 10^{-1} A.

The possibility of spontaneous currents in carbon nanotori has been studied by Sasaki and Kawazoe.¹² However, the origin of these currents is different than in our case. The spontaneous currents in Ref. 12 are of geometrical origin and appear only in twisted tori. The spontaneous current investigated in the present paper is a result of the interaction between currents from individual shells of the MWNT, and can be strongly enhanced by doping.

When the currents from subsequent shells are diamagnetic, they shield the external magnetic field and we may obtain at least a partial flux expulsion. The possibility of field and flux expulsion and flux trapping in mesoscopic cylinders consisting of a set of conductive sheets has been investigated in Ref. 5, for the systems in which the Fermi surface has large flat parts, like in (B) and (C) nanotubes. The results obtained in that paper can be used to discuss the field expulsion in MWNT's.

The configuration (C) is the one in which all active zig-zag shells display currents of diamagnetic character. Using

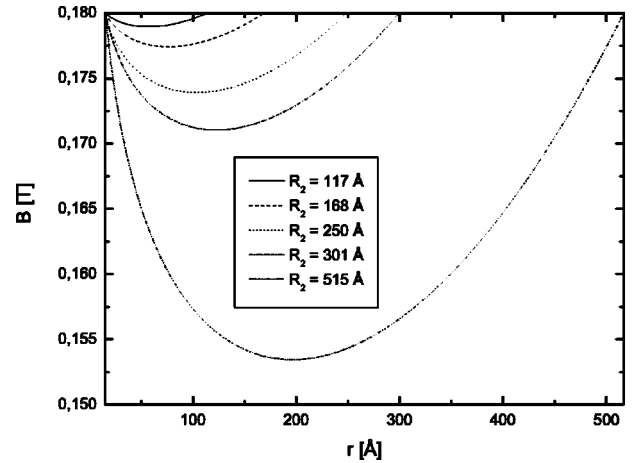


FIG. 8. The field expulsion in the MWNT as a function of the distance from the nanotube axis, for several numbers of active sheets.

the technique developed in Ref. 5 we performed the calculation of the magnetic field $B(r)$ inside the MWNT whose inner radius is $R_1 = 15 \text{ \AA}$ for different values of the outer radius R_2 , i.e., for different numbers of active shells. We assumed that the distance between active shells $b = 3 \cdot 3.4 \text{ \AA} = 10.2 \text{ \AA}$, and the lattice constant in the shell is 1.42 \AA . The results of these calculations, showing a decrease of the magnetic field inside the CN are presented in Fig. 8.

The curves in Fig. 8 represent the field expulsion for MWNT's with inner radius $R_1 = 15 \text{ \AA}$, and outer $R_2 = 117, 168, 250, 301, 515 \text{ \AA}$, respectively. The field expelled from the thinnest nanotube is of the order of 1% of the external field, while for the thickest MWNT (with the greatest number of active shells) it reaches 15%.

VI. CONCLUSIONS

Persistent currents in MWNT's are a superposition of currents from the component shells. We investigated tubes in different chirality configurations and found that in many of them currents in the shells are small and/or add destructively, resulting in a very small net current. However we have shown that there also exist some configurations in which the currents both are large and add coherently, resulting in enhanced effective currents.

The total magnetic field is then the sum of the external field and the one induced by the currents. It raises the possibility of investigating collective phenomena such as spontaneous currents and flux expulsion. We found three optimal configurations [labeled as (A), (B), and (C)] for which the currents were largest.

In cases (A) and (B) we found a small spontaneous current, due to the sawtooth shape of the $I(\phi)$ characteristics.

The MWNT's of type (C) exhibit some flux expulsion. This effect increases with the thickness of the sample—in the thickest considered sample we obtained a 15% reduction of the field due to a Meissner-type effect.

To our knowledge the largest MWNT's fabricated nowadays have the diameter of the order of 240 nm (thickness of the order of 100 nm),¹³ however, they are very dirty. That is why we have not included them into our considerations. Nevertheless, in light of the tremendous progress in the synthesis of carbon materials there is a possibility that relatively clean nanotubes of that thickness may become available and we estimate that in those the field expulsion may reach 50%.

Due to their curious magnetic properties the MWNTs may find many applications in magnetoelectronics, e.g., as magnetic sensors or nanotransistors. The effect presented in this paper, if confirmed experimentally, may open a way for vari-

ous applications of MWNTs connected with nanoelectronics, like logical circuits or memory storage devices.

ACKNOWLEDGMENTS

This work was supported by the Polish Committee for Scientific Research (KBN) Grant No. P03B 033 20. M.S. acknowledges the support of the Polish Ministry of Scientific Research and Information Technology under the (solicited) Grant No. PBZ-MIN-008/P03/2003. E.Z. acknowledges the support of the EC Contract No. RITA-CT-2003-506095.

¹*Carbon Nanotubes - Synthesis, Structure, Properties and Applications*, edited by M. S. Dresselhaus, G. Dresselhaus, and P. Avouris (Springer-Verlag, Berlin, 2001).

²M. Szopa, M. Margańska, and E. Zipper, *Phys. Lett. A* **299**, 593 (2002).

³M. Szopa and E. Zipper, *Int. J. Mod. Phys. B* **9**, 161 (1995); D. Wohlleben, M. Esser, P. Freche, E. Zipper, and M. Szopa, *Phys. Rev. Lett.* **66**, 3191 (1991).

⁴J. Wang and Z.-S. Ma, *Phys. Rev. B* **52**, 14 829 (1995); T. V. Shahbazyan and S. E. Ulloa, *Physica E (Amsterdam)* **1**, 259 (1997).

⁵M. Czechowska, M. Lisowski, M. Szopa, and E. Zipper, *Phys. Rev. B* **68**, 035320 (2003).

⁶M. Krüger, M. R. Buitelaar, T. Nussbaumer, and C. Schön-

berger, *Appl. Phys. Lett.* **78**, 1291 (2001).

⁷C.-H. Kiang, M. Endo, P. M. Ajayan, G. Dresselhaus, and M. S. Dresselhaus, *Phys. Rev. Lett.* **81**, 1869 (1998).

⁸S. Roche, F. Triozon, A. Rubio, and D. Mayou, *Phys. Lett. A* **285**, 94 (2001).

⁹E. Jouguelet, C. Mathis, and P. Petit, *Chem. Phys. Lett.* **318**, 561 (2000).

¹⁰S. Roche and R. Saito, *Phys. Rev. Lett.* **87**, 246803 (2001).

¹¹H.-F. Cheung, Y. Gefen, E. K. Riedel, and W.-H. Shih, *Phys. Rev. B* **37**, 6050 (1988).

¹²K. Sasaki and Y. Kawazoe, cond-mat/0307339 (unpublished).

¹³J.-B. Park, G.-S. Choi, Y.-S. Cho, S.-Y. Hong, D. Kim, S.-Y. Choi, J.-H. Lee, and K.-I. Cho, *J. Cryst. Growth* **244**, 211 (2002).